Multi-scale fibre-based optical frequency combs: science, technology and applications (MEFISTA)

Deliverables D1.1 Numerical model for few mode fibre ring cavities

Project details

Project Number	861152	Project Acronym	MEFISTA
Project Title	Multi-scale fibre-based optical frequency combs: science, technology and applications		
Project website	https://mefista.astonphotonics.uk/		
Starting date	01/02/2020		
Project duration	48		
Call (part) identifier	H2020-MSCA-ITN-2019		
Topic	MSCA-ITN-2019 Innovative Training Network		

Document details

Title	Numerical model for few mode fibre ring cavities		
Deliverable number	D1	Deliverable Rel. number	D1.1
Work Package	WP1		
Deliverable type	Report		
Description	Numerical model for few mode fibre ring cavities		
Deliverable due date	31st January 2021		
Actual date of submission	13th February 2023		
Lead beneficiary	ULille		
Version number	V1.0		
Status	Public, Final		

Dissemination level

Public (PU)	X
Confidential, only for members of the consortium (including Commission Services)	

Contents

Numerical model for few-mode fibre ring cavities

A fiber ring cavity is a common type of resonator composed by a piece of fiber close into itself with an optical coupler. Two of the most common way to describe such systems are the Ikeda MAP and Lugiato-Lefever Equation (LLE) models.
In the following report we provide a description of these models generalized for our case of study (Gain Through Filtering). In conclusion, we provide some examples of their application such as parametric gain calculation and numerical simulations.

The Ikeda map model:

This model was first proposed by Ikeda [1], and contextualized in our specific subject takes the following form [2]:

$$i\,\frac{\partial A_n}{\partial z} - \frac{\beta_2}{2}\,\frac{\partial^2 A_n}{\partial t^2} + \gamma |A_n|^2 A_n = 0\,, 0 < z < L, \qquad (1)$$

$$A_{n+1}(z=0,t) = \theta E_{IN} + \rho e^{i\phi_0} A_n(z=L,t). \qquad (2)$$

In eq. (1) is described the evolution of the envelope of the field $A_n(z,t)$ in its n_{th} roundtrip of the cavity: z measures the position of the field inside the cavity, which has a total length of L, t is the retarded time. β_2 accounts for the group velocity dispersion, and γ is the Kerr non-linearity coefficient.
Being a cavity, the model is completed with the boundary conditions described in eq. (2): E_{IN} is the input field, injected trough the coupler which has a reflectivity of ρ and a transmittance of θ . In this case, all the losses are lumped into ρ, so that $1-\rho^2$ accounts for the overall power losses in a roundtrip. $\phi_0 = \beta(\omega_p)L\ (mod\ 2\pi)$ is the linear phase shift per roundtrip modulo $2\,\pi$.

In our specific case the cavity includes a filter in the form of a Fiber Bragg Grating (FBG), and considering that it can be placed at the position $z = z_F$, we can write:

$$A_n(z_F^+,t) = h(t) \star A_{n(z_F^-,t)}, (3)$$

$$\hat{A}_{n(z_F^+,\omega)} = H(\omega)\hat{A}_n(z_F^-,\omega), (4)$$

Where $h(t)$ represent the impulse response of the filter, and $H(\omega)$ is its transfer function. By assuming that the filter is placed just before the coupler ($z_F = L$), it's possible to rewrite the boundary conditions as:

$$A_{n+1}(z=0,t) = \theta E_{IN} + \rho e^{i\phi_0}\, h\,(t) \star A_n(z=L,t), \qquad (5)$$

$$\hat{A}_{n+1}(z=0,\omega) = \theta E_{IN}\delta(\omega) + \rho e^{i\phi_0} H(\omega)\hat{A}_n(z=L,\omega), \qquad (6)$$

Where $\delta(\omega)$ is the Dirac delta function.

The filter is described through the following model [2]:

$$H(\omega) = e^{F(\omega)+i\psi(\omega)}, \qquad (7)$$

$$F(\omega) = b\frac{a^4}{(\omega-\omega_f)^4 + a^4}, \qquad (8)$$

$$\psi(\omega) = ba\frac{(\omega-\omega_f)[(\omega-\omega_f)^2 + a^2]}{\sqrt{2}\,[(\omega-\omega^4) + a^4]}, \qquad (9).$$

Equations (8) and (9) describes the loss profile and the phase of the filter respectively, the parameter a is related to the filter bandwidth (rad/s), while the parameter b is a non dimensional number which controls the maximum attenuation of the filter.

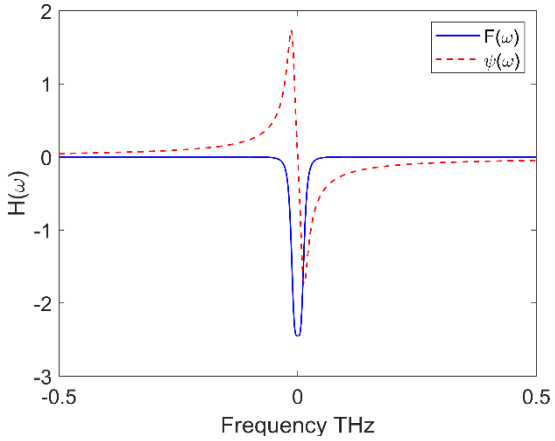

Fig. 1: Typical response of the filter with the model described by Eqs. (8) and (9). $a = 85e^9 rad/s$, $b = -2.45$, $w_f = 314\ GHz$.

Steady State and Stability Analysis of the Ikeda map model

The stationary, CW solutions are in the following form:

$$A_n(z,t) = \bar{A}\, e^{i\,\gamma P\, z}, P = |\bar{A}|^2.$$

From the stationary state solutions, it' relation between the input and the field circulating inside the cavity:

$$\bar{A} = \frac{\theta}{1-\rho e^{i\,\phi} H(0)}\, E_{IN}, \qquad (10)$$

$$P = \frac{\theta^2}{1+\rho^2|H(0)|^2 - 2\,\rho|H(0)|\cos\,(\phi+\psi(0))} P_{IN}, \qquad (11)$$

Where $\phi = \phi_0 + \gamma PL$ account for the total phase accumulated by the signal during the propagation inside the cavity, $\psi(0)$ is the phase of the filter at the pump frequency, $|H(0)|$ is the losses imposed

by the filter at the pump frequency, and E_{IN}, P_{IN} are the amplitude and power of the pump field, respectively.
By performing a linear stability analysis, which consist in the linearization and diagonalization of the system described by Eqs. (1) and (5) [2], it's possible to calculate a gain function. That function allows to predict the frequency and the power grow rate of the perturbations destabilized inside the cavity. In other words, if a given frequency ω_i gives a gain $g_{MAP}(\omega_i) \neq 0$, then the power of the perturbation at frequency ω_i will grows as $\exp(g_{MAP}(\omega_i)z)$.
It's then possible formulate the gain for the Ikeda map model as:

$$g_{MAP}(\omega) = \frac{2}{L}\ln\max\{|\lambda_1, \lambda_2|\}. \quad (12)$$

Where $\lambda_{1,2} = \frac{\Delta}{2} \pm \sqrt{\frac{\Delta^2}{4} - W}$ are the eigenvalue of the system which describe the propagation of the perturbation inside the cavity and:

$$\Delta = \rho\left[2\cos(k\,L)\left(H_e(\omega)\,cos\phi - H_{o(\omega)}\,sin\phi\right) - \frac{\beta_2\omega^2+2\gamma P}{k}\sin(kL)(H_{o(\omega)}\cos\phi + H_e(\omega)sin\phi)\right] \quad (13)$$

$$W = \rho^2(H_e(\omega)^2 + H_o(\omega)^2\,), \qquad (14)$$

with $H_e(\omega), H_o(\omega)$ being the even and odd part of the filter's transfer function $H(\omega)$, and $k(\omega) = \sqrt{\frac{\beta_2\omega^2}{2}\left(\frac{\beta_2\omega^2}{2} + 2\,\gamma P\right)}$ being the wave number of the perturbation. Some examples of gain calculation are provided in the following sections.

Lugiato-Lefever Equation model:

The Lugiato-Lefever Equation (LLE) is another model which allow to describe the dynamic of a fiber ring cavity, and other types of resonators [3].
This model is calculated under the assumption that the envelope of the field propagating inside the cavity doesn't change much during a single round-trip. This is equivalent to assume that the overall losses of the cavity are small ($\rho \approx 1, \theta \ll 1$), in what is called the *good cavity limit*.
This mean-field model, can be computed by performing a suitable averaging of the Ikeda map of Eqs. (1) and (5), which reads [2]:

$$L\frac{\partial A}{\partial z} = [-\alpha + i\,\phi_0 + \Phi\star + i\,\Psi\star]A + \left[-\frac{iL\beta_2}{2}\frac{\partial^2}{\partial t^2} + i\,L\,\gamma|A|^2\right]A + \theta\sqrt{P_{IN}}. \qquad (14)$$

Where Φ and Ψ being the Fourier anti-transform of Eqs. (8) and (9) respectively.

Steady State and Stability Analysis of the LLE model

As for the Ikeda map model, it's possible to compute the relation between the input and the intracavity power by considering the field homogeneous inside the cavity ($\frac{\partial}{\partial z} = \frac{\partial}{\partial t} = 0$), and then find the relation between the intracavity power and the input power as:

$$\bar{P} = \frac{\theta^2}{\left(-\alpha + F(0)\right)^2 + (\phi_0 + \psi(0) + \gamma L\,\bar{P})^2}P_{IN}. \quad (15)$$

By linearizing and diagonalizing the model, it's possible to compute the gain function as:

$$g_{LLE}(\omega) = 2\frac{-\alpha + F_{e(\omega)} + Re(\lambda_+)}{L}, \qquad (16)$$

$$\lambda_\pm = \pm\sqrt{(-[\mu(\omega) - iF_o(\omega)]^2 + (\gamma L\,\bar{P})^2)}\,, \qquad (17)$$

With $\mu = L\frac{\omega^2\beta_2}{2} + 2\,\gamma\,\bar{P}L + \phi_0 + \psi_e(\omega)$ being a phase-mismatch factor and $F_e(\omega), F_o(\omega)$ are the even and odd part of $F(\omega)$, the function describing the loss profile of the filter as described in Eq. (8).

Examples of Gain and comparison between Ikeda and LLE models

In this section we show some examples of calculation of the gain with the model described previously.
Figs. 2(a) and 2(b) depict the evolution of the gain as function of the input power for the Ikeda and LLE models, respectively. Only the positive gain tongue is displayed, as the negative one is symmetric. Is interesting to see the similarity between the two results in this situation.
Figs. 3(a) and 3(b) show the evolution of the gain, again for Ikeda and LLE model respectively, as function of the shift between the pump wavelength and the filter's central wavelength. Once again, the two 2D plot are quite similar. It's interesting to note the dependency of the gain bands position from the distance of the pump-filter wavelength shift. This opens the way to applications such as tunable frequency combs source [4].
In example of Figs 4(a) and 4(b), we report the evolution of the gain computed with Ikeda and LLE model, as function of the linear detuning $\delta = -\phi_0$. In this case we can see the real difference between the two models: the Ikeda model, Fig. 4(a), is periodic as function of the detuning, while the LLE, Fig. 4(b), is not. This is due to the nature of the Ikeda and LLE models: the first one is a strict representation of the real-world cavity, periodic in space domain and thus also in the linear phase. On the other hand, the LLE is a mean-field model averaged on one round-trip, which lose the information about this periodicity. The mathematical representation is lighter but, to be accurate, the model has to be used withing the assumption made for the model derivation (good cavity limit).
Figs 5 is example of numerical integration, through a split-step-Fourier method: Fig. 5(a) is a plot of the time domain signals, blue for LLE and red for Ikeda map model, and Fig. 5(b) are the relative spectra. It is possible to see a good qualitative agreement but, despite being well inside the good cavity limit ($\rho = \sqrt{0.9}$, $\theta = \sqrt{0.1}$), it's possible to note a slight difference in the repetition of the spectra and the amplitude of the time domain signal.

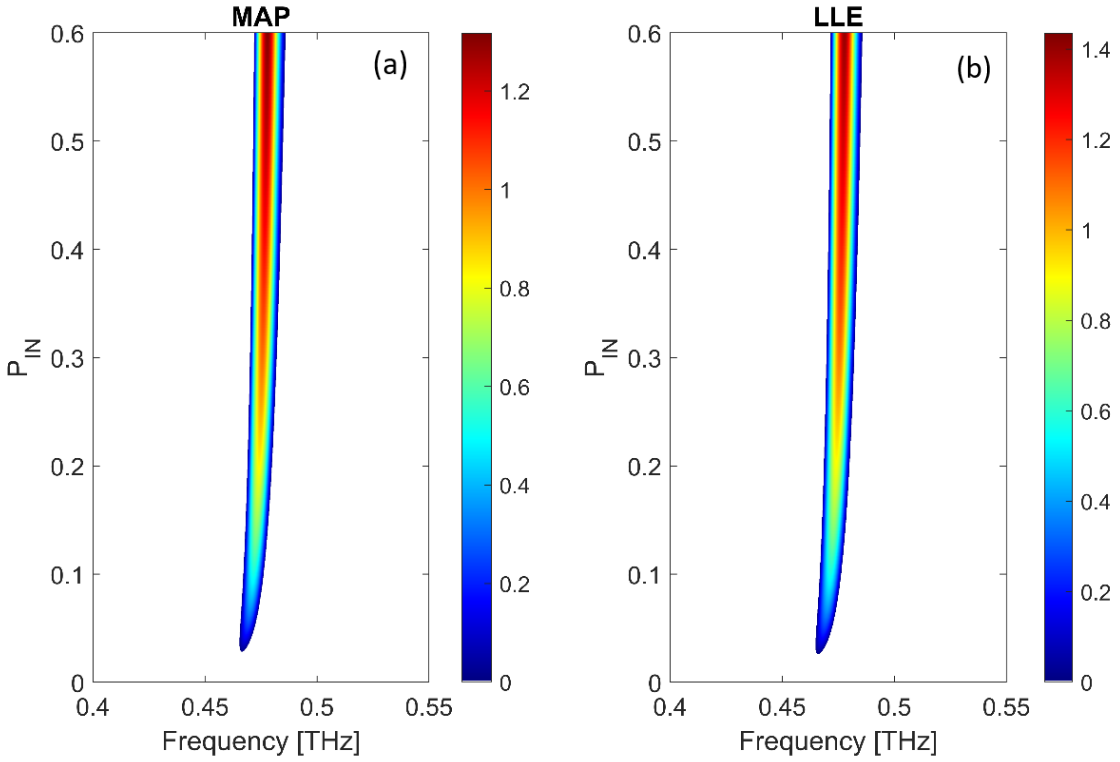

Fig.2 (a) Evolution of the gain computed with the Ikeda map model Eq. (12) as function of input power P_{IN} . (b) Evolution of the gain computed with LLE model, Eq. (16) as function of input power P_{IN}. For both calculation the same parameter has been used: $\beta_2 = 0.5ps^2km^{-1}, \gamma = 2.5W^{-1}km^{-1}, L = 100m, \rho = \sqrt{0.9}, \theta = \sqrt{0.1}, \phi_0 = -\psi(0), a = 85\frac{rad}{ns}$ $b = -2.45,$ $\omega_f = 314\,GHz.$

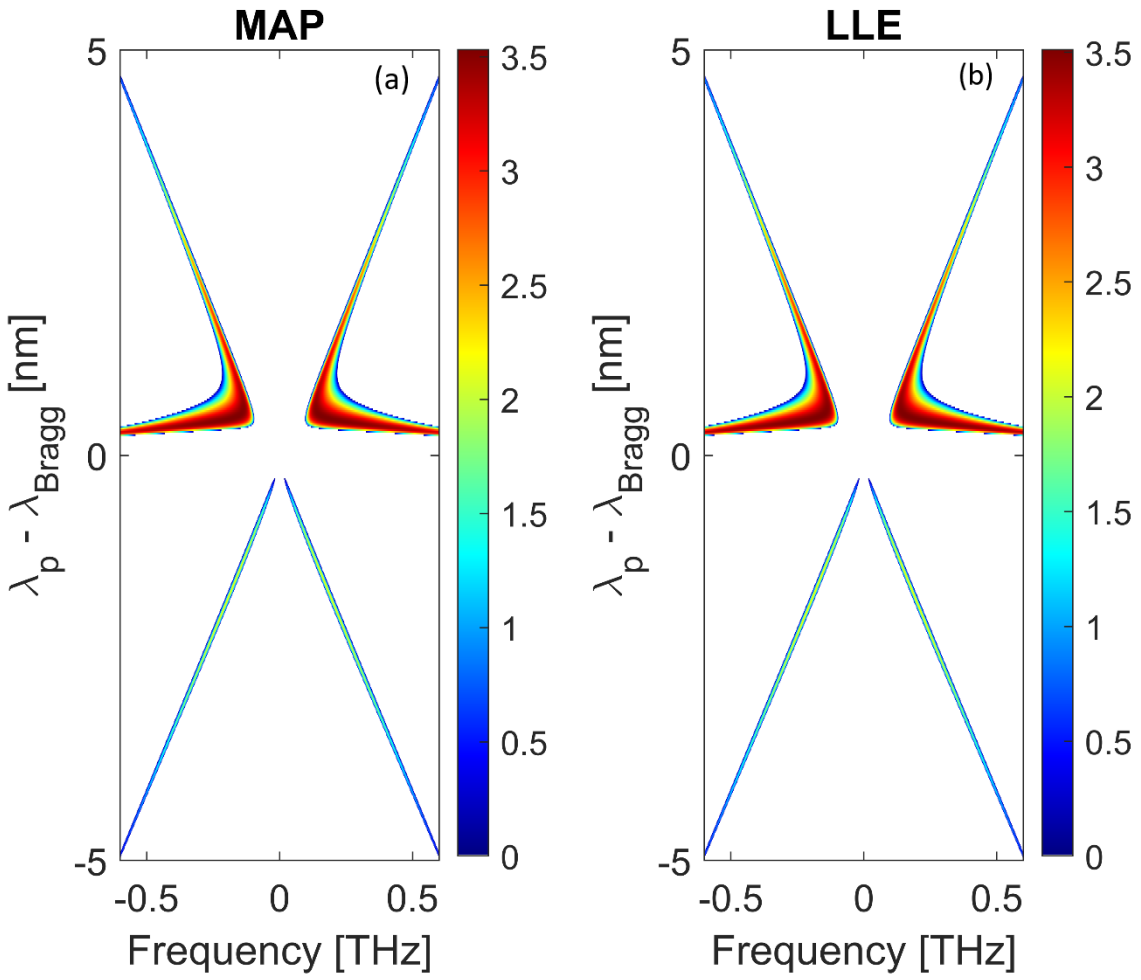

Fig.3 (a) Evolution of the gain computed with the Ikeda map model Eq. (12) as function of the wavelength shift between the pump, λ_p , and the filter λ_{Bragg} . (b) The same kind of evolution of the gain, computed with LLE model Eq. (16). For both calculation the following parameter has been used: $\beta_2 = 0.5ps^2km^{-1}, \gamma = 2.5W^{-1}km^{-1}, L = 100m, \rho = \sqrt{0.9}, \theta = \sqrt{0.1}, \phi_0 = -\psi(0), a = 85\frac{rad}{ns}$ $b = -2.45,$ $\omega_f = 314\,GHz,$ $P_{IN} = 0.5W$. In both cases the wavelength of the pump is shifted in a $\pm 5\ nm$ interval from the central wavelength of the filter λ_{Bragg}.

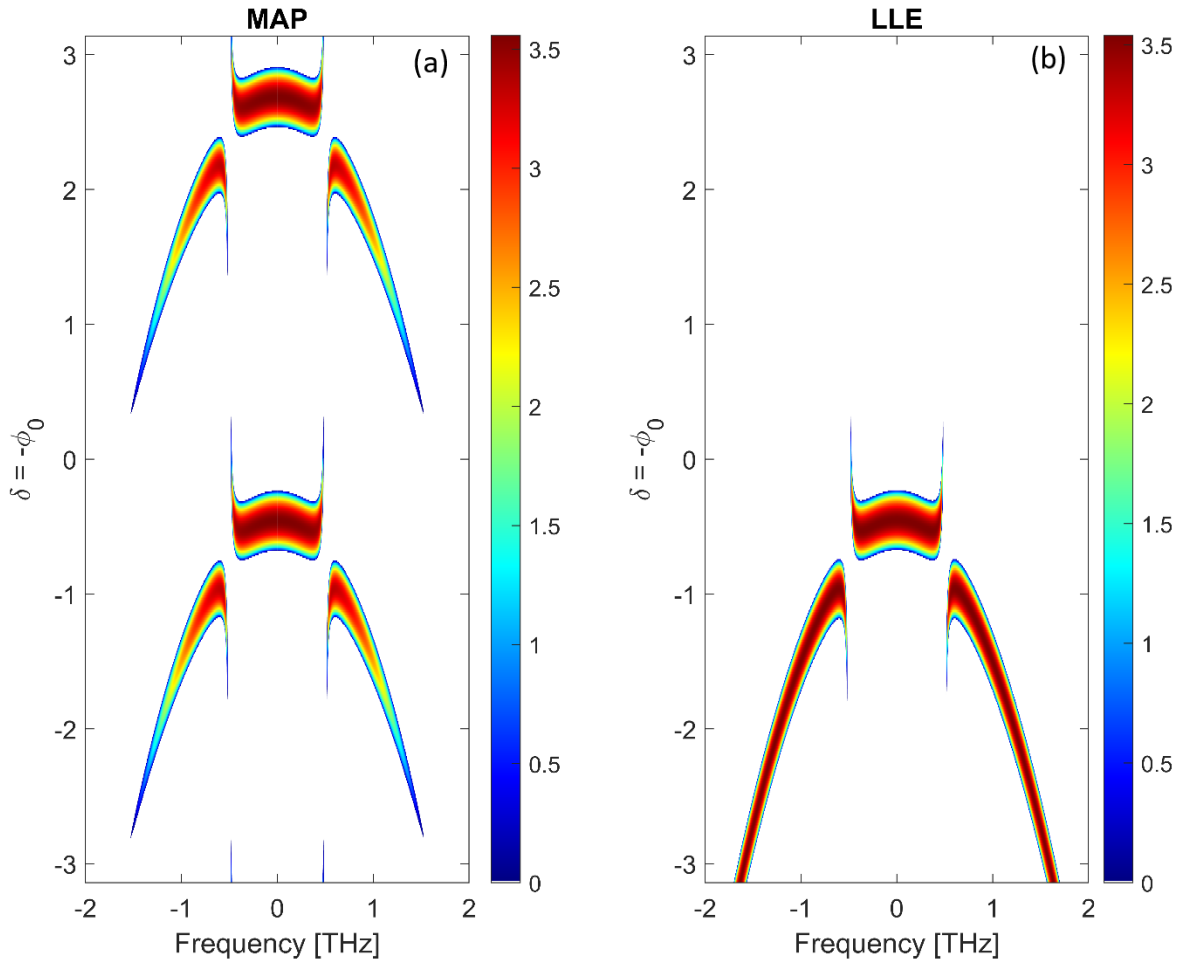

Fig.4 (a) Evolution of the gain computed with the Ikeda map model Eq. (12) as function linear phase detuning $\delta = -\phi_0$. (b) Evolution of the gain computed with LLE model, Eq. (16) function linear phase detuning $\delta = -\phi_0$. The parameters for the calculations are: $\beta_2 = 0.5ps^2km^{-1}, \gamma = 2.5W^{-1}km^{-1}, L = 100m,\ \rho = \sqrt{0.9}, \theta = \sqrt{0.1}, \phi_0 = -\psi(0), a = 85\frac{rad}{ns}\ b = -2.45,\ \omega_f = 314\ GHz, P_{IN} = 0.5W.$

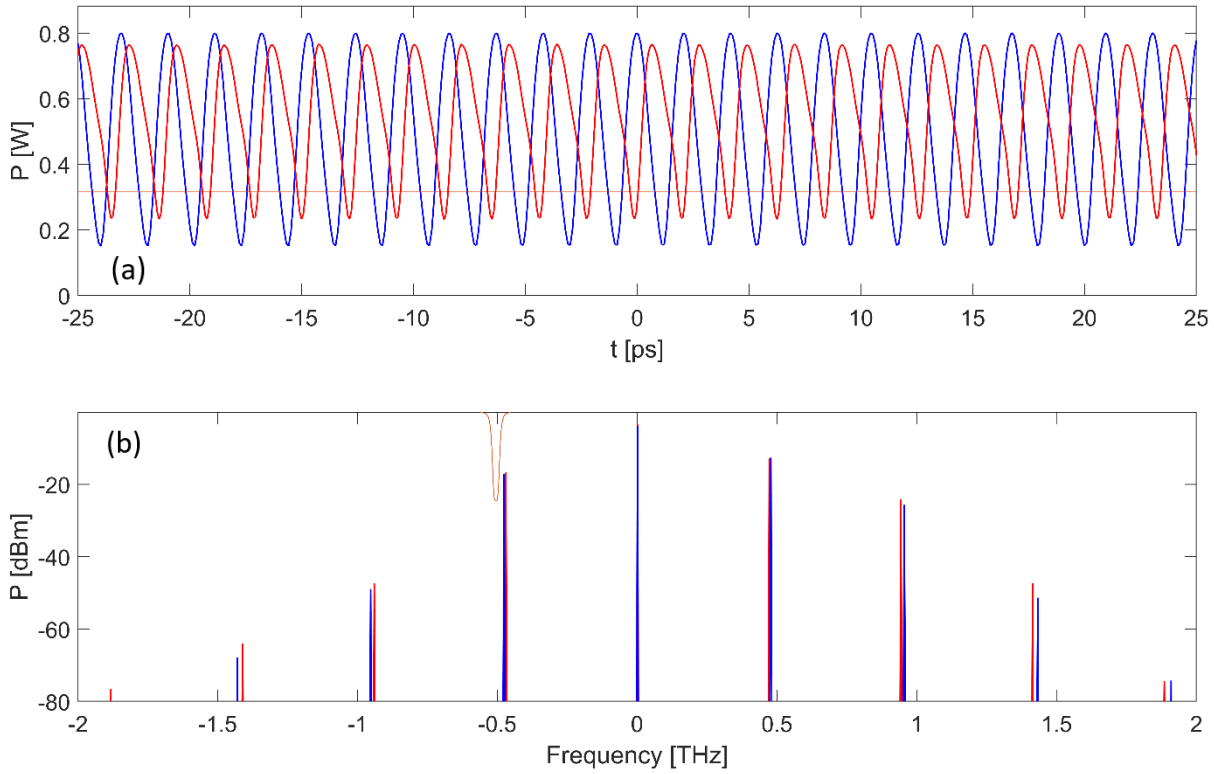

Fig. 5 (a) Temporal domain signals for Ikeda map (red) and LLE (blue) after a total propagation of 100 Km. The correspondent power spectra are showed in (b), the orange trace is the filters loss profile.
The parameters are: $:\beta_2 = 0.5ps^2km^{-1}, \gamma = 2.5W^{-1}km^{-1}, L = 100m, \rho = \sqrt{0.9}\,, \theta = \sqrt{0.1}\,, \phi_0 = -\psi(0), a = 85\frac{rad}{ns}\ b = -2.45,\ \omega_f = 314\ GHz, P_{IN} = 0.1W.$

Conclusion:

In this report we have presented the two main mathematical model used to describe few mode fiber ring cavities in the frame of GTF investigation. Then, a few examples which illustrate the Ikeda and LLE model are proposed, underlining common point and criticalities of the two, before an example of numerical integration.
This theoretical framework is very flexible and, in the future, will be expanded two the more complex case of PM fiber cavities.

Reference:

[1]

K. Ikeda, 'Multiple-valued stationary state and its instability of the transmitted light by a ring cavity system', *Optics Communications*, vol. 30, no. 2, pp. 257–261, Aug. 1979, doi: 10.1016/0030-4018(79)90090-7.

[2]

A. M. Perego, A. Mussot, and M. Conforti, 'Theory of filter-induced modulation instability in driven passive optical resonators', *Phys. Rev. A*, vol. 103, no. 1, p. 013522, Jan. 2021, doi: 10.1103/PhysRevA.103.013522.

[3]

L. A. Lugiato and R. Lefever, 'Spatial Dissipative Structures in Passive Optical Systems', *Phys. Rev. Lett.*, vol. 58, no. 21, pp. 2209–2211, May 1987, doi: 10.1103/PhysRevLett.58.2209.

[4]

F. Bessin *et al.*, 'Gain-through-filtering enables tuneable frequency comb generation in passive optical resonators', *Nature Communications*, vol. 10, no. 1, Art. no. 1, Oct. 2019, doi: 10.1038/s41467-019-12375-3.

This Project has received funding from the European Union's Horizon 2020 research and innovation programme under the Marie Sklodowska-Curie grant agreement No 861152